A Comparison of Reconstructed Ku-band Scatterometry, C-band Scatterometry, and SSM/I Imagery for Tropical Vegetation Classification

Perry J. Hardin[1], David G. Long[2], Quinn P. Remund[2], and Douglas R. Daum[2]
Microwave Earth Remote Sensing Group
690 SWKT, Brigham Young University, Provo, Utah 84602
Phone: 801-378-6062 Email: perry_hardin@byu.edu, david_long@byu.edu

I. LOW-RESOLUTION MONITORING OF EARTH

In support of efforts to detect and measure global climate and landcover change, remotely sensed imagery is frequently employed. Because these monitoring efforts are truly *global*, low-resolution sensors are frequently preferred over high resolution Landsat and SPOT sensors. For example, Advanced Very High Resolution Radiometer (AVHRR) imagery and its derivative vegetation indices are utilized for inexpensive low-resolution monitoring of equatorial forests where high-resolution imaging with Landsat-type satellites would be inappropriate.

The AVHRR instruments that flew on polar orbiters NOAA-7, NOAA-9 and NOAA-11 were five-channel radiometers capable of continuously scanning the earth with 1 km ground resolution. While these 1 km data are available for limited portions of Earth, AVHRR global area coverage (GAC) data are resampled on-board the satellite to 4 km resolution and stored for later transmission. The popular global vegetation index products derived from GAC data are further resampled to resolutions between 13 km and 26 km. The two AVHRR channels typically used for vegetation inventory include:

1. 0.58 to 0.68μm
2. 0.725 to 1.10μm

In contrast to AVHRR, *microwave* radiometers are electromagnetic receivers which measure radiation in the frequency band of 1-300 Ghz. Microwave radiometers have proven invaluable for collecting global geophysical information. The Special Sensor Microwave / Imager (SSM/I), part of the Defense Meteorological Satellite Program, has been used to measure cloud water content, precipitation, snow cover, and surface temperature. Currently two SSM/I instruments are operational. SSM/I is a seven channel, four frequency radiometer. The frequencies include:

1. 19.35 Ghz, Vertical and horizontal polarizations
2. 22.235 Ghz, Vertical polarization only
3. 37.0 Ghz, Vertical and horizontal polarizations
4. 85.5 Ghz, Vertical and horizontal polarizations

The 3dB footprint for the SSM/I ranges from 13 to 69 km -- it is dependent on frequency and direction (along-track vs. cross-track).

Whereas microwave radiometers are passive, satellite scatterometers are active microwave instruments originally designed to measure the radar backscatter of the ocean's surface under all-weather conditions. The first spaceborne scatterometer flew as part of the Skylab missions. Between June and October of 1978, the Seasat-A Scatterometer (SASS) was able to obtain nearly continuous global, dual polarization Ku-band coverage at a spatial unit cell resolution of 50 km for nearly 100 days. The European Space Agency (ESA) successfully launched its ERS-1 satellite into a quasi-polar mission-adjustable orbit in the summer of 1991. The instrument payload included the Active Microwave Instrument (AMI) which is capable of operating in a vertically polarized wind scatterometer mode (5.3 Ghz) for the production of 50 km resolution cell wind vector products. Other scatterometer launches are planned.

With the exception of AVHRR, the primary mission of all the instruments described has been the remote sensing of the earth's atmosphere and ocean. This is not surprising, because most land imaging applications require spatial resolutions finer than the footprints appropriate for large ocean expanses or atmospheric sounding. However, a new multivariate image reconstruction technique [1] has improved the resolution of imagery produced by SASS, the ERS-1 scatterometer, and SSM/I to resolutions between 5 and 20 km, making them candidates for medium-scale monitoring of cloudy global areas such as the Arctic, Antarctic, and continental equatorial forests. Furthermore, successful efforts have been made to remove atmospheric distortion in the SSM/I data [2].

One goal of the research reported in this paper is to combine these reconstructed image data sets with AVHRR vegetation index images for discriminating between vegetation formations in central South America. This also provides an opportunity to compare the utility of the various image types for equatorial vegetation discrimination in general.

[1] Department of Geography
[2] Department of Electrical and Computer Engineering

0-7803-3068-4/96$5.00©1996 IEEE

II. METHODOLOGY

Reconstruction of SASS imagery is discussed elsewhere [1]. The reconstructed image used for this project (Figure 1), was composited from data collected over central South America from July 1 to October 10, 1978. Only vertically polarized data acquired with incidence angles between 23° and 55° degrees with noise below a certain predetermined level were used. Additionally, orbits for which the spacecraft attitude determination were in error were excluded.

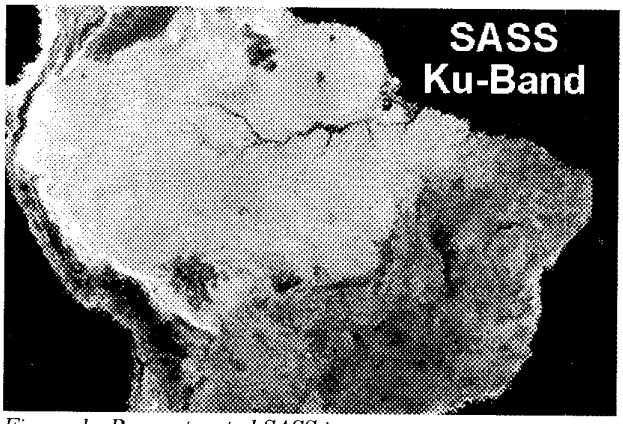

Figure 1. Reconstructed SASS image.

In order to maximize the fairness of any comparison with SASS (which had a limited life), an NDVI composite was constructed for the same seasonal period, albeit in 1982 (Figure 2). This was the earliest AVHRR imagery available. The process of creating the NDVI composite has already been described [3].

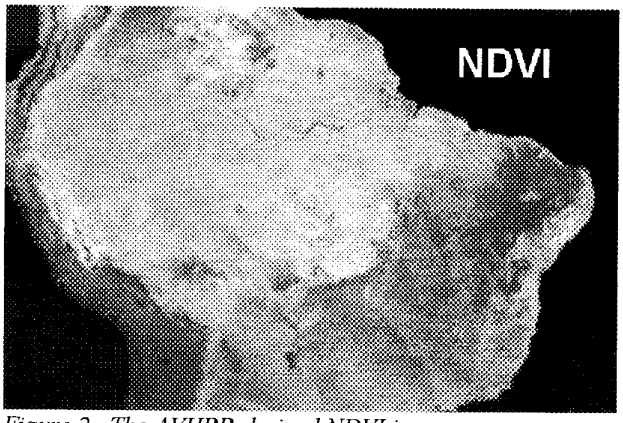

Figure 2. The AVHRR-derived NDVI image

The SSM/I data used in this project was acquired during September of 1992. Since SSM/I has seven channels, seven images were reconstructed. A discussion of the SSM/I reconstruction process is reported in these proceedings [4] and will not be repeated here. The images used in this research are also available in that reference.

Discriminating between equatorial vegetation using reconstructed ERS-1 imagery is also reported in these proceedings [5] for the interested researcher to review. Although ERS-1 data for that research was acquired between April, 1992 and May, 1995, only the data from July 1 through September 30, 1992 were composited for this project -- roughly the seasonal time-frame associated with the SASS imagery.

Since all the images were reconstructed to differing resolutions between 5 and 20 km, the images were all resampled to the lowest common resolution (20 km), cast to a common projection using nearest neighbor resampling, and registered.

A simple experiment was devised to test the utility of the reconstructed imagery and AVHRR for discrimination between broad vegetation classes within the study area of central South America. Using the 1:5,000,000-scale *Vegetation Map of South America* [6], large homogeneous rectangular regions for 15 different vegetation formations were delimited. A total of 21 rectangular regions were delineated, totaling over 566,000 km^2. Once these regions were defined, the pixels from the SSM/I, SASS, ERS-1 and NDVI images were extracted for each and saved for further analysis. In the discrimination to be described next, only one-third of the pixels for each of the 15 formations were used for training. The remaining two-thirds were reserved for testing the discrimination.

To establish a baseline estimate of discrimination ability, there was an initial analysis to classify the 15 vegetation formations using linear discriminant functions generated from the training set classes. After the baseline classification was established, the original 15 categories were regrouped into a set of 10 categories to improve the accuracy. This was done primarily by combining the forest formations.

To limit the complexity of the iterative discrimination, we selected only one SMM/I band to include with the SASS, ERS-1 and NDVI images. From initial tests, we found the 85H channel to be slightly superior to the others for discriminating between the vegetation classes. It was used in the discrimination analysis.

Since the goal of this research is to combine these data sets and compare them for discrimination of vegetation, all possible combinations of ERS-1, SASS, NDVI and SSM/I 85H were tried in the experiments in order to find the optimum combination for classification. Coefficients for Fisher's linear discriminant function were generated using the training data. The functions were then applied to each pixel in the test data set. Accuracy was assessed by counting the number of pixels in each vegetation class which were correctly classified by the discriminant

functions. The results were also summarized in confusion matrices.

III. RESULTS

The average image values for the 15 original classes are shown in Table 1. Variance values, some substantial, are not shown in order to conserve space. In general, there is agreement in trend between the values. The equatorial forests have the highest backscatter, while the shrublands and grasslands have the lowest.

As shown in Table 2, the best single image for classifying the 15 vegetation classes is ERS-1. However, the performance of all the single images is abysmal, with accuracy ranging from 22% to 30%. When two images are used together, the highest classification accuracy is obtained when 85H is combined with either ERS-1 or NDVI (51% - 52%). As might then be expected, when ERS-1 is combined with both NDVI and 85H, the accuracy increases further (63%). Using all four images produces an accuracy of 67%. For the sake of comparison, we also report that the classification accuracy using the seven SSM/I channels alone is 61%. When all ten images are utilized together, the classification accuracy exceeds 74%.

Grouping the forest classes substantially improves the classification accuracy, as does grouping two *campos cerrados* classes. The trend in the discrimination analyses for the ten collapsed groups follows the pattern established for the previous experiment. Using SASS, ERS-1, NDVI, and 85H together produces an accuracy of 90%. When the experiment is repeated with all seven SSM/I bands, the classification accuracy increases significantly to 93%.

IV. CONCLUSION

Given the results of the discrimination experiments, the following conclusions can be made.

1. Reconstructed radiometer imagery appears to have greater potential for discriminating between equatorial vegetation than either reconstructed C-band or Ku-band imagery.
2. Reconstructed C-band imagery is only slightly better than reconstructed Ku-band imagery for vegetation discrimination when combined with other reconstructed image types.
3. Use of all possible reconstructed images achieves the highest possible classification accuracy.
4. The different forest classes are difficult to distinguish between, although easily distinguishable from non-forest classes.

Perhaps the most intriguing aspect of the discrimination analysis is the superior value of reconstructed SSM/I imagery for distinguishing between equatorial vegetation. Clearly more research is warranted in SSM/I reconstruction.

Vegetation Formation	SASS A	ERS-1 A	NDVI	85H K
Very moist forest	-7.7	-8.1	0.29	286.1
Moist seasonal forest	-7.5	-8.0	0.29	287.2
Ombrophilous submontane forest	-7.5	-7.9	0.29	284.4
Extremely moist forest	-7.2	-7.7	0.28	286.1
Tropical seasonal lowland forest	-7.8	-8.2	0.28	287.1
Degraded forest formation	-7.6	-8.0	0.26	282.6
Degraded deciduous woodland	-8.6	-9.0	0.25	288.8
Campos sujos / limpos	-10.14	-10.4	0.19	288.7
Campos cerrados south	-10.9	-11.1	0.18	280.6
Chaco	-9.5	-9.7	0.16	283.8
Campos cerrados north	-10.0	-10.3	0.15	286.4
Degraded lowland woodlands	-10.7	-10.8	0.15	**
Degraded *campos cerrados*	-11.18	-11.3	0.14	280.0
Degraded *caatinga* formation	-9.8	-10.0	0.09	286.3
Caatinga	-9.3	-9.6	0.08	286.1

Table 1. Mean values for the 15 vegetation classes.
*** Unavailable at publication time.*

Images used	Accuracy %
NDVI	21.6
SASS	23.8
85H	24.2
ERS-1	29.8
SASS, ERS-1	40.0
ERS-1, NDVI	48.6
SASS, 85H	48.9
SASS, NDVI	49.1
ERS1, 85H	51.1
NDVI, 85H	51.5
SASS, ERS-1, NDVI	53.8
SASS, ERS-1, 85H	58.7
SASS, NDVI, 85H	58.8
ERS-1 NDVI, 85H	62.8
SASS, ERS1, NDVI, 85H	66.7
Seven SSM/I channels alone	60.9
SASS, ERS1, NDVI, seven SSM/I channels	74.4

Table 2. Results from the 15 group discrimination analysis.

V. REFERENCES

[1] D.G. Long, P.J. Hardin, and P.T. Whiting, "Resolution enhancement of spaceborne scatterometer data," IEEE. Trans. Geo. Remote Sensing, vol. 31, no.3, pp. 700-715, 1993.

[2] D. Daum, "Application of enhanced resolution imaging to SSM/I data," M.S. Thesis, Department of Computer and Electrical Engineering, Brigham Young University, 1994.

[3] P.J. Hardin and D.G. Long, "Integrating reconstructed scatterometer and Advanced Very High Resolution Radiometer data for tropical forest inventory," Optical Engineering, vol. 34, no. 11, pp. 3146-3153.

[4] D.G. Long, D.L. Daum, and P.J. Hardin, "Spatial resolution enhancement of SSM/I data: vegetation studies of the Amazon Basin," Proceedings, IGARSS '96, Lincoln Nebraska, May, 1996.

[5] P.J. Hardin, D.G. Long, and Q.P. Remund, "Discrimination of Africa's vegetation using reconstructed ERS-1 imagery," Proceedings, IGARSS '96, Lincoln Nebraska, May, 1996.

[6] UNESCO. "Vegetation map of South America," Paris: UN Educational, Scientific, and Cultural Organization, 1981.